1-1-2013

Ash2 acts as an ecdysone receptor coactivator by stabilizing the histone methyltransferase Trr.

Albert Carbonell
Departament de Genètica, Institut de Biomedicina, Universitat de Barcelona

Alexander Mazo
Department of Biochemistry and Molecular Biology, Thomas Jefferson University, Alexander.Mazo@jefferson.edu

Florenci Serras
Departament de Genètica, Institut de Biomedicina, Universitat de Barcelona

Montserrat Corominas
Departament de Genètica, Institut de Biomedicina, Universitat de Barcelona

Ash2 acts as an ecdysone receptor coactivator by stabilizing the histone methyltransferase Trr

Albert Carbonell[a], Alexander Mazo[b], Florenci Serras[a], and Montserrat Corominas[a]
[a]Departament de Genètica and Institut de Biomedicina, Universitat de Barcelona, 08028 Barcelona, Spain;
[b]Department of Biochemistry and Molecular Biology, Thomas Jefferson University, Philadelphia, PA 19107

ABSTRACT **The molting hormone ecdysone triggers chromatin changes via histone modifications that are important for gene regulation. On hormone activation, the ecdysone receptor (EcR) binds to the SET domain–containing histone H3 methyltransferase trithorax-related protein (Trr). Methylation of histone H3 at lysine 4 (H3K4me), which is associated with transcriptional activation, requires several cofactors, including Ash2. We find that *ash2* mutants have severe defects in pupariation and metamorphosis due to a lack of activation of ecdysone-responsive genes. This transcriptional defect is caused by the absence of the H3K4me3 marks set by Trr in these genes. We present evidence that Ash2 interacts with Trr and is required for its stabilization. Thus we propose that Ash2 functions together with Trr as an ecdysone receptor coactivator.**

Monitoring Editor
A. Gregory Matera
University of North Carolina

Received: Apr 6, 2012
Revised: Oct 3, 2012
Accepted: Nov 20, 2012

INTRODUCTION

The ecdysone receptor is a nuclear hormone receptor found in invertebrates and consists of a noncovalent heterodimer of two proteins—the ecdysone receptor (EcR) and ultraspiracle (USP; Oro *et al.*, 1990; Koelle *et al.*, 1991; Christianson *et al.*, 1992; Yao *et al.*, 1992). On ecdysterone (20E) binding, the ecdysone receptor triggers all molting transitions of the larvae and many of the events that occur during metamorphosis (Berger and Dubrovsky, 2005). A prerequisite for the transcriptional regulation of ecdysone-dependent genes is the nuclear localization of EcR/USP and its interaction with specific DNA sequences—the hormone response elements (Vogtli *et al.*, 1998). Although previous reports show that ecdysone receptor binds DNA constitutively and associates with either coactivators or corepressors depending on their status of ligand binding (Dressel *et al.*, 1999; Tsai *et al.*, 1999; Bai *et al.*, 2000; Beckstead *et al.*, 2001; Sedkov *et al.*, 2003; Gates *et al.*, 2004; Badenhorst *et al.*, 2005; Francis *et al.*, 2010), a recent study shows that, in the absence of the hormone, both EcR subunits localize to the cytoplasm, and the heme-binding nuclear receptor E75A replaces EcR/USP at common target sequences in several genes (Johnston *et al.*, 2011).

Whereas *usp* encodes a single protein product (Henrich *et al.*, 1990; Oro *et al.*, 1990; Shea *et al.*, 1990), *EcR* encodes three isoforms that differ in their N-terminal sequences: EcR-A, EcR-B1, and EcR-B2 (Talbot *et al.*, 1993). Differential expression of these isoforms dictates the tissue specificity of ecdysone responses in developing *Drosophila* (Talbot *et al.*, 1993). For example, EcR-A is predominantly expressed in imaginal cells, which contribute to adult structures, whereas EcR-B1 is predominantly expressed in larval cells, which are committed to die after larval stages.

Changes in chromatin organization and histone modifications are crucial for gene activation mediated by nuclear receptors. One such modification is methylation of lysine residues, which can carry multiple methyl groups (Eissenberg and Shilatifard, 2010; Justin *et al.*, 2010). Lysine methylation requires complexes that contain proteins with the SET domain, a conserved sequence first recognized in three *Drosophila melanogaster* proteins: Su(var)3-9, E(z), and trithorax (Trx; Tschiersch *et al.*, 1994). Histone H3 lysine 4 methylation (H3K4me) is mostly driven by type 2 histone lysine methyltransferases (KMT2; Allis *et al.*, 2007), which contain proteins of the Set1/COMPASS in yeast (Miller *et al.*, 2001; Roguev *et al.*, 2001; Nagy *et al.*, 2002), the trithorax group (TrxG), the trithorax-related (Trr), and the dSet1 proteins in flies (Sedkov *et al.*, 2003; Smith *et al.*, 2004; Papp and Muller, 2006; Ardehali *et al.*, 2011; Mohan *et al.*, 2011), and the mixed-lineage leukemia family (MLL1-5, Set1A/B) in mammals (Milne *et al.*, 2002; Goo *et al.*, 2003; Wysocka *et al.*, 2003;

This article was published online ahead of print in MBoC in Press (http://www.molbiolcell.org/cgi/doi/10.1091/mbc.E12-04-0267) on November 28, 2012.
Address correspondence to: Montserrat Corominas (mcorominas@ub.edu).
Abbreviations used: 20-HE, 20-hydroxyecdysone; AEL, after egg laying; Ash2, absent, small, or homeotic disks 2; BR-C, broad; ChIP, chromatin immunoprecipitation; E75A, ecdysone-induced protein 75B; EcR, ecdysone receptor; H3K4me3, trimethylation of histone H3 at lysine 4; lcp9, larval cuticle protein 9; rp49, ribosomal protein L32; sply, sphingosine-1-phosphate lyase; Trr, trithorax-related; Trx, trithorax; TSS, transcription start site; Usp, ultraspiracle.

Supplemental Material can be found at:
http://www.molbiolcell.org/content/suppl/2012/11/26/mbc.E12-04-0267v1.DC1.html

Hughes *et al.*, 2004; Yokoyama *et al.*, 2004; Lee and Skalnik, 2005; Lee *et al.*, 2006, 2007; Ruthenburg *et al.*, 2007). Trimethylation of H3K4 (H3K4me3) is associated with transcriptionally active regions (Dillon *et al.*, 2005; Eissenberg and Shilatifard, 2010) and is a conserved mark of chromatin at nucleosomes immediately downstream of promoters of transcribed genes (Pokholok *et al.*, 2005; Barski *et al.*, 2007; Guenther *et al.*, 2007; Schuettengruber *et al.*, 2009; Perez-Lluch *et al.*, 2011). Trx is the prototypical *Drosophila* member of the TrxG family. In line with the TrxG function, loss-of-function mutations of *trx* cause homeotic transformations in embryos and larvae (Ingham, 1983; Breen and Harte, 1991). TrxG and MLL proteins have been found in numerous complexes in different organisms (Shilatifard, 2008), and analysis of polytene chromosomes in flies show that the number of sites that accumulate H3K4me3 is greater than can be attributed to these individual proteins, indicating nonredundant activities (Eissenberg and Shilatifard, 2010). Trr is a KMT2 similar to Trx (Sedkov *et al.*, 1999). *Trr* mutants, however, do not display homeotic changes but instead interact with EcR, indicating that Trr functions as a coactivator of EcR by altering the chromatin structure at ecdysone-responsive promoters (Sedkov *et al.*, 2003).

The *ash2* gene, a member of TrxG, was discovered in a screen for mutants in *Drosophila* with imaginal disk abnormalities (Shearn *et al.*, 1971; Shearn and Garen, 1974). Loss-of-function mutations of this gene cause homeotic transformations and down-regulation of Hox genes (LaJeunesse and Shearn, 1995), in addition to several abnormalities, such as reduction of intervein and enhancement of vein tissues in the wing (Adamson and Shearn, 1996; Amoros *et al.*, 2002; Angulo *et al.*, 2004). The Ash2 protein is similar to two subunits of the COMPASS complex in yeast—Bre2 (Cps60) and Spp1 (Cps40; Roguev *et al.*, 2001; Krogan *et al.*, 2002; Steward *et al.*, 2006). Biochemical and RNA interference studies have identified the mammalian orthologue of Ash2, ASH2L, to be a core subunit of KMT2 complexes that is required for H3K4me3 (Dou *et al.*, 2006; Steward *et al.*, 2006; Southall *et al.*, 2009; Cao *et al.*, 2010), and nucleosome Western blots and clonal analysis indicate that Ash2 is also necessary for H3K4me3 in *Drosophila* (Beltran *et al.*, 2007).

Here we show that Ash2 is required for pupariation and metamorphosis, playing a role in the transcriptional activation of ecdysone-responsive genes by promoting H3K4me3. By investigating the relationship of Ash2 with KMT2s in several *Drosophila* tissues, we also provide evidence that Ash2 is involved in the stabilization of the EcR coactivator Trr.

RESULTS

ash2 mutants affected ecdysone-triggered biological responses

Flies homozygous for the $ash2^{l1}$ allele have reduced and abnormal imaginal disks and brain, and this is lethal in late third instar (Amoros *et al.*, 2002; Beltran *et al.*, 2003; Angulo *et al.*, 2004). At this stage, wandering $ash2^{l1}$ mutant larvae stopped moving and became extended and stiff in an apparent attempt to pupariate. Defects associated with ecdysteroid signaling became apparent. Ninety-seven percent of animals did not evert their anterior spiracles or displayed defects in this eversion (Figure 1, A and B). Moreover, $ash2^{l1}$ mutant larvae did not undergo body shortening or sticking to the wall to enter into prepupa stage, phenomena that normally occur before metamorphosis; instead, they remained in larval stage for 6 extra days before dying. Homozygous mutants of the hypomorphic allele $ash2^{1124.11}$ displayed similar, although milder, phenotypes (5.2% of spiracle eversion defects). Approximately 12% of $ash2^{1124.11}$ homozygous flies developed into sterile adults, which are known to survive for 2 d (Amoros *et al.*, 2002); however, some of them died during metamorphosis, with defects in ecdysone-triggered biological responses such as the head eversion (6%; Figure 1, C and D).

Failure in anterior spiracle eversion, a nonpupariating phenotype, and/or defects during metamorphosis are hallmarks of mutations in the loci associated with ecdysteroid signaling (Li and Bender, 2000; Bashirullah *et al.*, 2007; Francis *et al.*, 2010). To test whether *ash2* interacts with *EcR*, we analyzed the phenotype of double mutants. Two sets of evidence suggest that both proteins act in common processes. First, compared with $ash2^{1124.11}$, we obtained fewer flies carrying the EcR^{M554fs} and $ash2^{1124.11}$ alleles that were capable of completing metamorphosis (1.3% of survival, $n = 78$, as compared with 17.9% of survival, $n = 76$; Figure 1J). Heterozygous flies for either of the mutant alleles used as a control did not present any viability defects. Second, because Ash2 and EcR play a role in wing morphogenesis (D'Avino and Thummel, 2000; Amoros *et al.*, 2002; Angulo *et al.*, 2004), we also checked the adult wings of $EcR^{M554fs}/+$; $ash2^{1124.11}$ flies. Although only a small number of double mutants survived, they displayed an enhancement of the $ash2^{1124.11}$ wing phenotype. For example, in addition to the extra cross-vein defects, mutant wings displayed an aberrant shape not observed in either $EcR^{M554fs}/+$ or $ash2^{1124.11}$ mutants alone (Figure 1, E–I). Taken together, these results suggest that Ash2 and EcR are required for the viability and proper progression of the larvae through pupariation and metamorphosis events.

ASH2 is associated with EcR at the majority of ecdysone-responsive genes

To clarify the relationship between ASH2 and EcR, we compared their distribution on polytene chromosomes. Overlapping signals were observed in a significant fraction of binding sites for both proteins (Figure 2, A and B). In addition, we used data from recent genomic studies to compare the target genes of Ash2 and EcR. The Ash2 target genes were obtained by chromatin immunoprecipitation followed by high-throughput sequencing (ChIP-seq) in wing imaginal disk (Perez-Lluch *et al.*, 2011), whereas the EcR target genes were obtained by ChIP-Seq in white pupae (Roy *et al.*, 2010). Despite the differences in tissues and developmental stages, we found that 85% (361 genes) of the EcR target genes are also Ash2 target genes (Figure 2C). This strong overlap indicates that EcR and ASH2 cooperate in regulating a significant subset of ecdysone-responsive genes. Furthermore, the comparison with target genes previously obtained by ChIP-Seq of H3K4me3 in wing disk (Perez-Lluch *et al.*, 2011) suggests that 66% (239 genes) of these common target genes are indeed active in the third-instar wing imaginal disk. Gene Ontology (GO) analyses of the Ash2 and EcR common target genes showed that enriched categories are related to larval/pupal morphogenesis and metamorphosis (Figure 2D). This enrichment is expected for EcR function and reinforces the finding that Ash2 and EcR cooperate in pupariation and metamorphosis events.

We then analyzed the location of Ash2 and EcR in the genome by projecting the mean reads over the transcription start sites (TSS) of common target genes (Figure 2E). Although the Ash2 peak appears to be slightly displaced toward the 5′ side, both proteins, as well as H3K4me3, seem to occupy the same genomic region. This result suggests that EcR interacts with Ash2 to promote the activation of ecdysone-responsive genes.

Ash2-dependent H3K4 trimethylation at EcR target genes is required for their transcriptional activation

We next investigated the mRNA and protein levels of EcR in the absence of Ash2 in several tissues. Previously, in a comparative

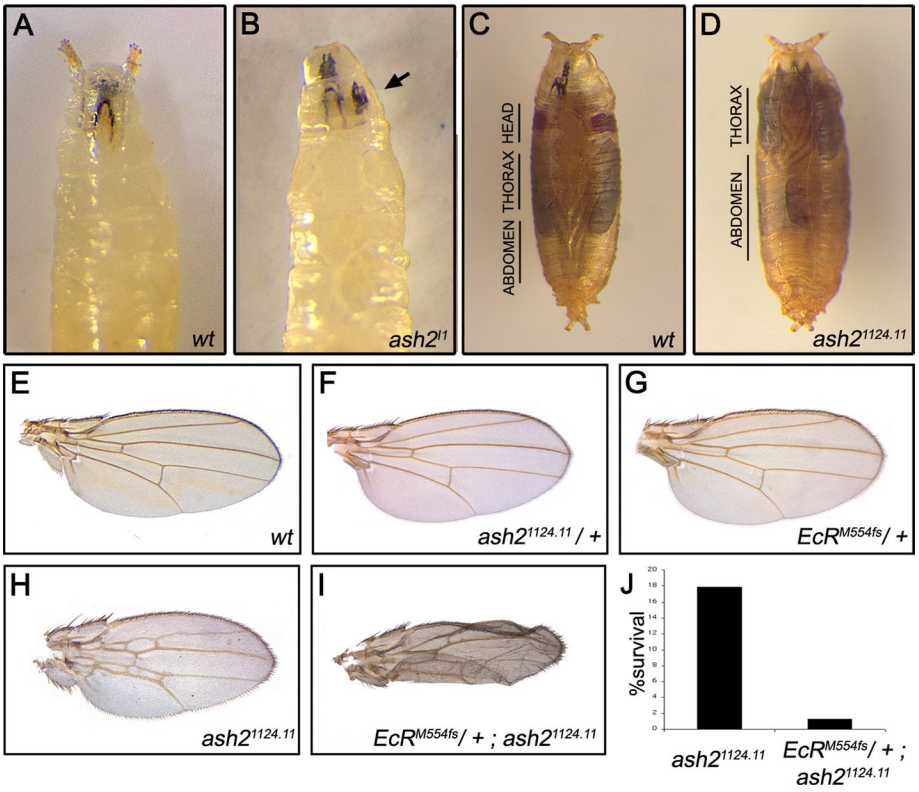

FIGURE 1: *ash2* mutants display defects in ecdysone-triggered biological responses. (A, B) Compared to wild-type, homozygous $ash2^{l1}$ late-wandering larvae displayed spiracle eversion defects (the noneverted necrotic anterior spiracle is indicated by arrow). (C, D) Ventral views show that $ash2^{1124.11}$ homozygous flies were "headless" as a result of failed head eversion and exhibited an elongated abdomen similar to the larval stage. (E–J) The combination of homozygous $ash2^{1124.11}$ with one copy of the EcR^{M554fs} allele led to a strong decrease in the percentage of animals that reached the adult state (1.3% of survival, $n = 78$, in Ecr^{M554fs}; $ash2^{1124.11}$ compared with 17.9% of survival, $n = 76$, in $ash2^{1124.11}$; J) and to an enhancement of the wing phenotype, with aberrant shapes and ectopic cross-veins apparent between L2–L3 and L4–L5 (H, I). All wings are shown at the same magnification.

expression analysis of wild-type and $ash2^{l1}$ wing disks, we detected similar transcript levels of EcR (289.7 in wild-type compared with 271.8 in $ash2^{l1}$ homozygous mutants (Beltran *et al.*, 2007)). Consistently, mutant clones of $ash2^{l1}$ induced 60 h after egg laying (AEL) in the wing disk showed no differences in the protein levels or in the subcellular localization of the EcR isoforms, neither in the peripodial membrane (where EcR-B1 is predominantly expressed; Figure 3A) nor in the columnar epithelium (where EcR-A is predominantly expressed; Figure 3B). Moreover, we did not observed changes in the level of EcR-A in $ash2^{l1}$ mutant disks compared with wild-type disks (Supplemental Figure S2). Thus EcR transcript and protein levels are not altered in *ash2* mutants. Similarly, no significant differences in the amount of the nuclear EcR protein were detected in mutant clones of trr^1 on salivary glands (Johnston *et al.*, 2011).

We hypothesized that if Ash2 and EcR work cooperatively, the absence of Ash2 may compromise the transcriptional activation of EcR-induced genes. To analyze this, we dissected fat bodies of wild-type and $ash2^{l1}$ late larvae before pupariation and performed reverse transcription (RT)-PCR for two of the early ecdysone-responsive genes that are also targets of Ash2 and EcR, namely *BR-C* and *E75A* (Gauhar *et al.*, 2009; Perez-Lluch *et al.*, 2011). We evaluated two biological replicates of RNA extracts and found a significant reduction in the levels of both *BR-C* and *E75A* in the $ash2^{l1}$ mutant tissue (Figure 3C). This result supports our previous microarray data in wing disks, which also showed a reduction of *BR-C* and *E75A* levels (wild-type vs. $ash2^{l1}$: 322.5 compared with 85.9 for *BR-C*, and 219.8 compared with 79.5 for *E75A*; Beltran *et al.*, 2007). This decrease of transcript levels in *ash2* mutants can be extended to other known early ecdysone–responsive genes (Supplemental Table S1), indicating that Ash2 may function as a coactivator of the EcR complex. To strengthen this observation, we analyzed the levels of H3K4me3 by ChIP–quantitative PCR (qPCR) of *BR-C* and *E75A* in wild-type and $ash2^{l1}$ mutant larvae. We found that, in the absence of Ash2, this activating histone mark was severely depleted (Figure 3D). These results are not due to a general change in nucleosome positioning, since we obtain the same reduction when we normalized against histone H3 (Supplemental Figure S2C).

Ash2 is a cofactor of the ecdysone receptor coactivator Trr

Because Ash2 does not contain a SET domain, which is necessary to catalyze the trimethylation of H3K4, we investigated whether it could function cooperatively with Trr, a known coactivator of EcR that binds EcR-USP, to facilitate the ecdysone-dependent transcriptional activation of target genes (Sedkov *et al.*, 2003). We analyzed for a putative relationship between Ash2 and Trr by several approaches. First, we investigated the phenotype of *trr* mutant clones in the adult fly. It has been shown that trr^1 clones result in malformations in the eye (Sedkov *et al.*, 2003), but no information has been provided for other tissues. We therefore used the same allele to study whether the phenotypes were similar to the ones observed in the *ash2*-mutant clones (Amoros *et al.*, 2002; Angulo *et al.*, 2004). Animals with trr^1 clones normally die if clones are induced early in development (60 ± 12 h AEL) but can survive if clones are induced later (85 ± 12 h AEL). In the wing, trr^1 clones (marked by *yellow*) were apparent only at the dorsoventral margin. These clones did not show the uniform polarized orientation of stout mechanosensory bristles but instead presented defects in bristle spacing and differentiation (Figure 4, A and B). This phenotype was highly penetrant (79.4% of the clones) and was similar to the anomalous arrangement of bristles of the wing margin of $ash2^{l1}$-mutant clones and to the aberrant bristle differentiation (partial ventralization of dorsal wing margin) of $ash2^{112411}$ homozygous flies described previously (Amoros *et al.*, 2002; Beltran *et al.*, 2007). We also explored the differentiation of mutant clones in the abdomen, which allows low-viability clones to be easily recovered, and found that trr^1 cells presented wild-type trichomes but lacked chaetes and macrochaetes in the abdominal *a4* and *a5* segments, respectively (Figure 4C). Thus the results from both wing and abdomen support a function for Trr in bristle development.

We next examined the genetic interaction between *ash2* and *trr*. Similar to *EcR* mutants, the combination of trr^1 with the hypomorphic

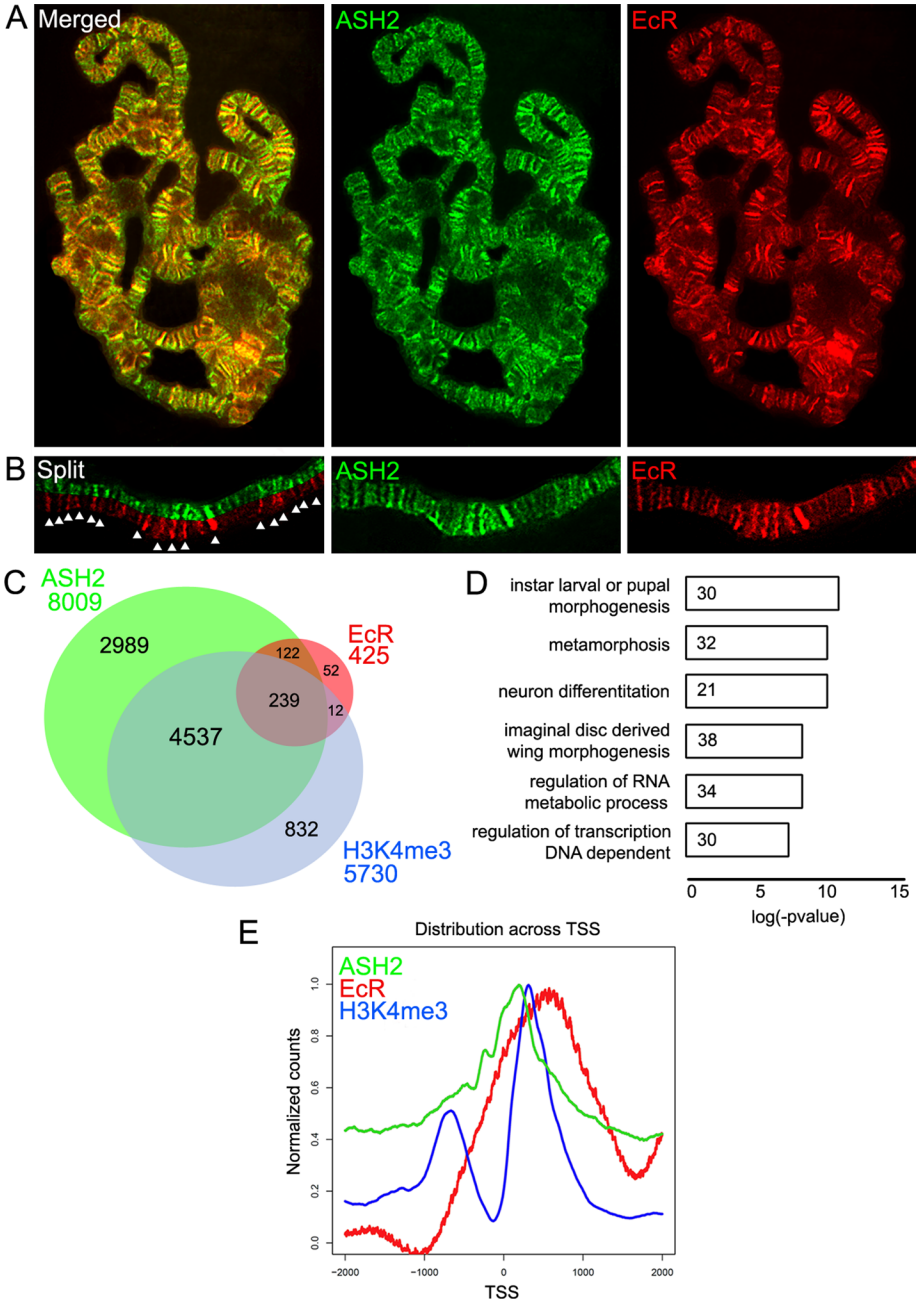

FIGURE 2: Ash2 associates with EcR at the majority of ecdysone-responsive genes. (A) Ash2 colocalized with EcR (EcR-B1) on polytene chromosomes from third-instar larvae. (B) Magnification of a chromosome arm shown in a split view. Arrows mark examples of overlapping bands. (C) Venn diagrams showing the intersection between Ash2, EcR, and H3K4me3 target genes. (D) GO term enrichment of target genes common to both Ash2 and EcR. (E) Projection of Ash2, EcR, and H3K4me3 ChIP-Seq reads over the TSS of their common target genes.

allele $ash2^{112411}$ resulted in a severe reduction of viability of $ash2^{112411}$ homozygous flies (3.4% in trr^{1}; $ash2^{1124.11}$, n = 60, compared with 17.9% in $ash2^{1124.11}$ mutants, n = 76; Figure 4D). Heterozygous flies for either of the mutant alleles used as controls did not present any viability defects. Wings of surviving flies also presented a more extreme phenotype, consisting of an aberrant shape, reduced wing size, partial fusion of the L2 and L3 veins, and massive intervein-to-vein transformation (Figure 4G). This phenotype was not observed for either the $trr^{1}/+$ or the $ash2^{1124.11}$ mutant alone (Figure 4, E and F). These results provide strong support for a functional relationship between the two genes.

In agreement with recently published results (Mohan *et al.*, 2011), coimmunoprecipitation experiments in embryos revealed a direct physical association of Ash2 with Trr (Figure 5A), providing additional support to the genetic finding of a functional relationship between Ash2 and Trr. These proteins were also observed to partially colocalize on salivary gland polytene chromosomes (Figure 5, B and C). The fact that additional bands were observed for Ash2 that did not overlap with Trr is consistent with the role of Ash2 as a coactivator for other histone methyltransferases.

Because Trr is recruited to the EcR-positive loci in response to ecdysone (Sedkov *et al.*, 2003; Johnston *et al.*, 2011), we next addressed whether Ash2 binding at the early ecdysone-induced puff 2B is also dependent on hormone treatment. Late larval and prepupal ecdysone pulses trigger a sequential induction of puffs in polytene chromosomes of salivary glands that correspond to loose chromatin structures where genes are actively transcribed. Early-responding puff 2B contains the *BR-C* gene, the expression of which depends on both Trr (Sedkov *et al.*, 2003) and Ash2 (Figure 3, C and D). Ash2 recruitment in response to ecdysone was analyzed after ectopic ecdysone treatment in salivary glands, which were dissected from mid-third-instar larvae and cultured at 25°C for 2 h either in the absence or in the presence of ecdysone. We found that raising the ecdysone levels in vivo resulted in an increased staining of Ash2 and EcR (Figure 6A) and of Trr and EcR (Figure 6B) in the 2B loci that was concomitant with puff formation. These observations support the idea that ecdysone signaling regulates Ash2 binding at EcR-positive targets.

Ash2 is required for Trr but not Trx stability

To clarify the functional relationship between Ash2 and Trr, we compared Trr distribution on the polytene chromosomes of wild-type and *ash2*-mutant larvae. The loss of Ash2 resulted in a significant reduction in the levels of Trr protein associated with polytene chromosomes (Figure 7A). A dramatic reduction of Trr nuclear levels was also detected by immunostaining in $ash2^{l1}$ clones in the wing disk (Figure 7B) and by Western blotting in nuclear extracts of $ash2^{l1}$ homozygous larvae (Figure 7C). To rule out that differences in protein content were due to changes at the RNA level, we performed RT-PCR experiments using third-instar larvae wing imaginal disks. We evaluated two biological replicates of RNA extracts from wild-type and $ash2^{l1}$ samples and found only a mild reduction of *trr* expression levels as compared with the internal control gene *sply* (Figure 7D). These results confirmed our previous

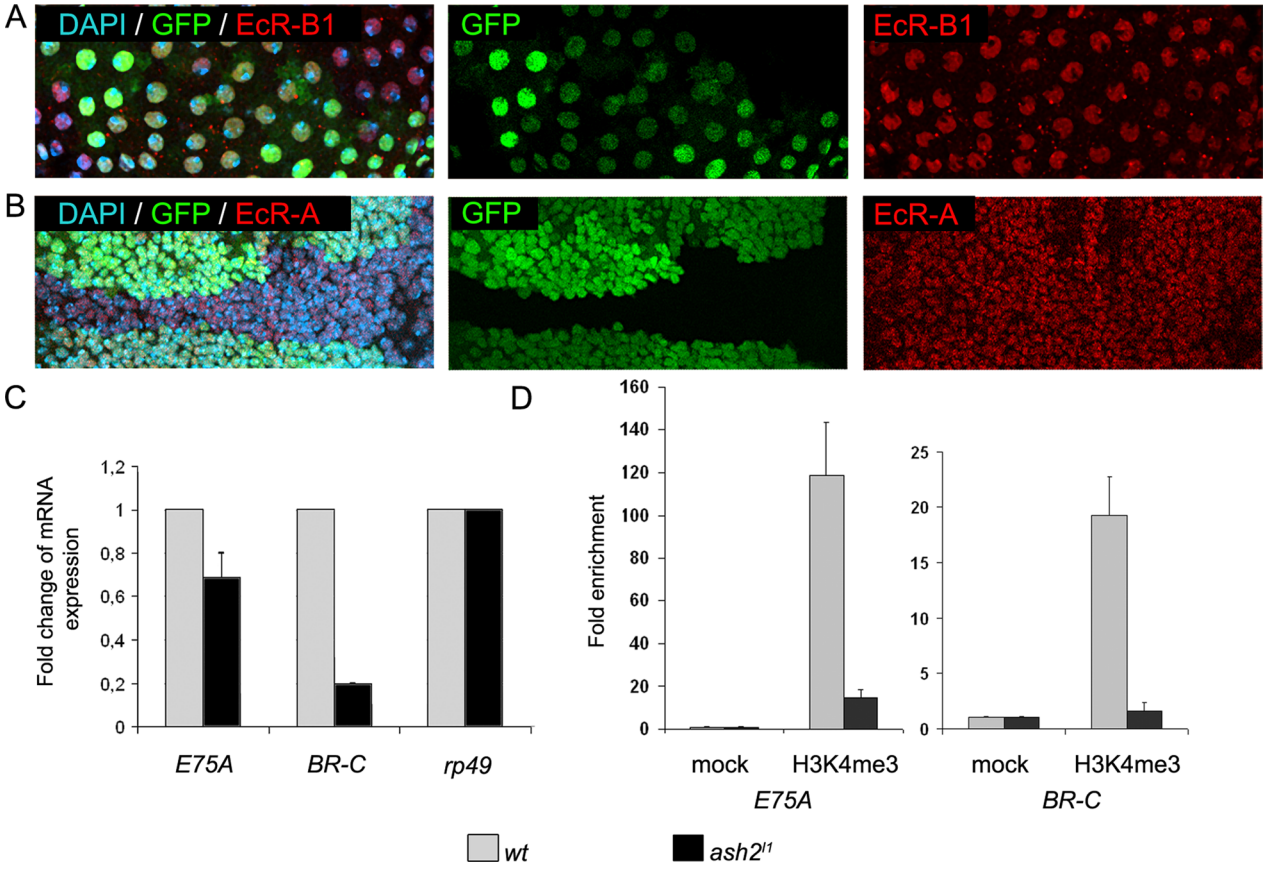

FIGURE 3: The Ash2 contribution to H3K4me3 levels at EcR target genes is required for their transcriptional activation. (A, B) Loss of Ash2 function did not reduce EcR levels. (A) Detection of EcR-B1 in wild-type (bright green), heterozygous (green), and *ash2*^{l1} homozygous (black) cells from the peripodial membrane of wing imaginal disk. (B) Detection of EcR-A in wild-type (bright green), heterozygous (green), and *ash2*^{l1} homozygous (black) cells from columnar epithelia of wing imaginal disk. (C) Effects of an *ash2* mutation on the expression of *BR-C* and *E75A*. Fat body mRNA levels of *BR-C* and *E75A* from late-wandering larva were measured by quantitative RT-PCR relative to *rp49*, used as a control. Error bars represent SEM. (D) ChIP analysis of wild-type and *ash2*^{l1} late-wandering larva with H3K4me3 antibody. The regions analyzed were the promoter region of *E75A* (of −1852 to −1751 from the TSS) and the 5′-untranslated region of *BR-C* (of +1079 to +1212 from the TSS). Real-time PCR results were normalized against the mock sample and are depicted as fold enrichment. Error bars represent SEM.

microarray analyses of wild-type and *ash2*^{l1} wing disks, from which we detected similar transcript levels of Trr (225.6 in wild-type compared with 219.6 in *ash2*^{l1} mutants; Beltran *et al.*, 2007).

Given that the mammalian orthologue of Ash2 (ASH2L) has been identified as a subunit of a core complex with several KMT2s (Dou *et al.*, 2006; Steward *et al.*, 2006; Southall *et al.*, 2009), we analyzed whether *Drosophila* Ash2 could play a general role in stabilizing other KMT2s, such as Trx. The physical interaction of Ash2 with Trx was determined by coimmunoprecipitation and immunostaining. By analyzing their distribution on polytene chromosomes, we found that Ash2 colocalized with Trx (Figure 8B) in a significant subset of bands, although, as expected, the number of chromosomal sites that accumulated Ash2 was greater that those with Trx. We also found Ash2 associated with the N-terminal cleaved form of Trx (Figure 8A), consistent with previous findings (Milne *et al.*, 2005; Mohan *et al.*, 2011).

We next assessed whether removing Ash2 would affect the Trx function. In contrast to our observations on Trr, the loss of *ash2* resulted in no major changes in the binding of Trx to polytene chromosomes (Figure 8C) or in the Trx levels in *ash2*^{l1}-mutant clones in the wing imaginal disk (Figure 8D), indicating the specificity of Ash2 function for Trr. Given that studies on the mammalian ASH2L and MLL1 have shown that ASH2L stimulates the catalytic activity of MLL1 (Dou *et al.*, 2006; Steward *et al.*, 2006; Southall *et al.*, 2009; Cao *et al.*, 2010), we next examined the effect of removing Ash2 on the H3K4me3 levels and Trx recruitment at specific genes. For this purpose, we performed ChIP experiments using antibodies against H3K4me3 and Trx at the *lcp9* gene. As expected, Trx was present in the absence of Ash2, but there was a severe drop of the H3K4me3 levels (Figure 8, E and F), suggesting that, as in mammals, Ash2 stimulates the catalytic activity of Trx. Taken together, our results confirm that Ash2 is a common partner for Trx and Trr KMT2s in *Drosophila* and reveal its specific role as a coactivator of EcR through stabilization of Trr.

DISCUSSION

In this work, we identified several *ash2* phenotypes that are characteristic for defects in ecdysone signaling, suggesting a critical role for Ash2 in ecdysone responses during late larval and pupal development. Two classes of genes are known to produce mutant phenotypes that resemble those seen in *ash2* mutant animals: those required for ecdysone biosynthesis or release (Garen *et al.*, 1977;

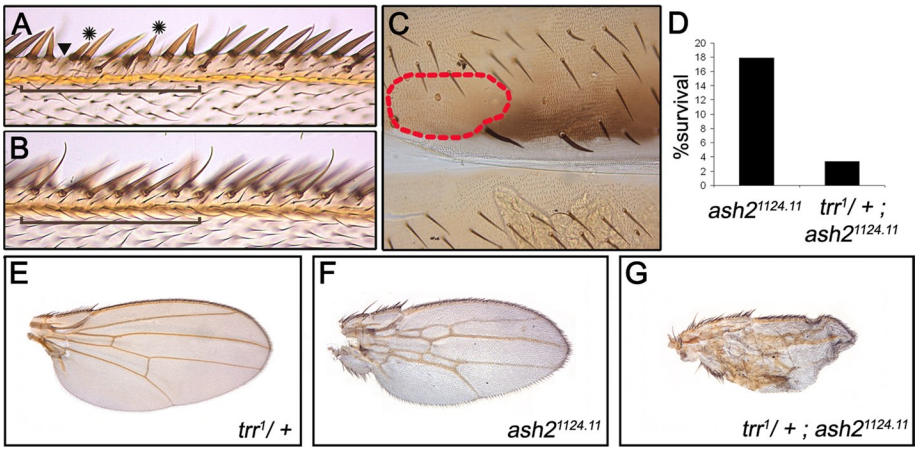

FIGURE 4: Wing and abdomen phenotypes of *trr mutants*. Dorsal (A) and ventral (B) views of the wing margin of *y trr*^{1} *FRT18A / w f*^{36a} *FRT18A; hs- FLP* adult flies. In the dorsal view, the *trr*^{1} mutant clone (␣) marked with *y* showed bristle-spacing defects (▼) and bristle-differentiation defects (✹). (C) Loss of chaetes and macrochaetes in the abdomen of a *trr*^{1} clone (┄), marked with *y*. (D–G) The combination of homozygous *ash2*$^{1124.11}$ with one copy of the *trr*^{1} allele strongly decreased the percentage of animals that reached the adult state (3.4% of survival, $n = 60$, in *trr*^{1}*; ash2*$^{1124.11}$ compared with 17.9% of survival, $n = 76$, in *ash2*$^{1124.11}$) and enhanced the *ash2*$^{1124.11}$ wing phenotype, with a reduction in wing size, a partial fusion of the L2 and L3 veins, and an increase of intervein-to-vein transformation (F, G). All wings are shown at the same magnification.

Venkatesh and Hasan, 1997; Freeman *et al.*, 1999), and those encoding nuclear receptors that mediate the ecdysone signal (Oro *et al.*, 1992; Bender *et al.*, 1997; Hall and Thummel, 1998; Schubiger *et al.*, 1998; Li and Bender, 2000; Bialecki *et al.*, 2002). We have now found that Ash2 functions as a coactivator of the ecdysone receptor in a significant subset of ecdysone-inducible genes and that it facilitates the Trr-induced H3K4me3 mark that is associated with transcriptional activation. *Ash2* mRNA expression peaks at white prepupae at 24 h, coinciding with a peak of expression of *EcR* (Roy *et al.*, 2010). This is in agreement with the nonpupariating phenotype observed in *ash2*^{l1} mutants and points to the importance of the Ash2 protein in the prepupal stages for regulating the entrance to pupariation and metamorphosis. Although younger larval molts also require EcR activity, *ash2* mutants did not seem to interfere with the early molts of earlier stages. In fact, *ash2* mutants are able to respond to the first third-instar pulse of ecdysone that induces larva to wander out of their food and begin pupating (King-Jones and Thummel, 2005). These results either suggest a differential requirement of Ash2 in EcR or reflect a strong maternal contribution of the Ash2 product. Because induction of EcR target genes is reduced but not completely abolished in *ash2*^{l1} mutants, we cannot exclude the possibility that lethality in the late third-instar stage reflects a differential sensitivity of various biological processes in the degree to which EcR is activated.

The change of H3K4me3 levels at EcR-inducible genes (*E75A* or *BR-C*) in *ash2* mutants indicates a role for Ash2 as an EcR coactivator. Moreover, Ash2 is required for the H3K4 trimethylation and the subsequent expression of *BR-C,* an early-ecdysone–responsive gene that is trimethylated on H3K4 by Trr (Sedkov *et al.*, 2003). The downregulation of this gene could explain the similar wing margin bristle defects observed in the *trr* and *ash2* mutants, since it has been reported that *BR-C* plays a role in controlling sensory neuron differentiation in the wing margin (Schubiger *et al.*, 2005). The more extreme wing phenotypes found in surviving flies from mutant combinations suggest that the expression of a subset of genes involved in wing morphogenesis is induced by an Ash2/Trr complex functioning as an EcR coactivator complex. In line with this, it has been reported that an ecdysone regulatory pathway controls wing morphogenesis and integrin expression during *Drosophila* metamorphosis (D'Avino and Thummel, 2000).

Our data confirm the role of Ash2 in promoting H3K4 trimethylation, as well as its function as a cofactor of the *Drosophila* Trx and Trr KMT2 proteins, supporting conservation between human and fly SET complexes. Our finding that Ash2 is a common partner of the *Drosophila* SET complexes is fully consistent with the recent characterizations of the dSET1 complex, which contains Ash2 (Ardehali *et al.*, 2011), and of the *Drosophila* COMPASS complexes, which contain Ash2 and are similar in their subunit composition to their mammalian counterparts (Mohan *et al.*, 2011). Both studies also showed that dSet1 is responsible for the majority of H3K4 dimethylation and trimethylation. In agreement with these and other reports (Dou *et al.*, 2006; Steward *et al.*, 2006), we observed a reduction of H3K4me3 and H3K4me2, but not of H3K4me1, upon depletion of ASH2 (Supplemental Figure S3), reinforcing a role for ASH2 as a general cofactor of this type of histone methyltransferase.

Nevertheless, our results demonstrate some specificity of the Ash2/Trr-induced H3K4me3 marking at ecdysone-responsive genes. With regard to the function of Ash2 in different SET complexes, it has been shown in *Saccharomyces cerevisiae* that inactivation of the Ash2 relative Bre2 did not affect the integrity of the complex but significantly impaired the catalytic activity of Set1 (Schneider *et al.*, 2005; Dehe *et al.*, 2006). Data from mammals revealed that this function is conserved, as ASH2L also stimulated the KMT2 activity of MLL1 (Dou *et al.*, 2006; Steward *et al.*, 2006; Southall *et al.*, 2009) and is involved directly with RbBP5 in the catalytic reaction by its ability to interact with H3 and *S*-adenosyl-L-[methyl-3H]methionine (Cao *et al.*, 2010). Given the highly conserved core configuration among the MLL/SET1 family of KMT2s and the global effects of ASH2L on H3K4 methylation, it has been proposed that this function could be a common feature for the regulation of other MLL/SET1 family members (Dou *et al.*, 2006; Cao *et al.*, 2010). Our results indicate that, in addition to its role in facilitating H3K4 trimethylation, Ash2 could play complex-specific roles. The depletion of Trr protein levels observed in *ash2* mutants points to a destabilization of Trr in the absence of Ash2, since only a mild reduction was observed at the RNA level that does not support transcriptional control. Several scenarios can explain this depletion. First, Ash2 may be required to stabilize Trr to chromatin upon EcR signaling and could subsequently contribute to its catalytic activity. Second, Ash2 could directly or indirectly control Trr synthesis or stability before binding to chromatin. There are several examples of chromatin-bound proteins that are degraded when released from chromatin (Li and DePamphilis, 2002; Sharma *et al.*, 2011). Although the proteosome pathway seems to play a role in the degradation of these, other mechanisms are also likely to be involved (Sharma *et al.*, 2011). Further experiments are necessary to address whether the mechanism involving Ash2-dependent Trr stabilization involves proteosomal degradation, but it is important to point out that Trr, similar to Trx,

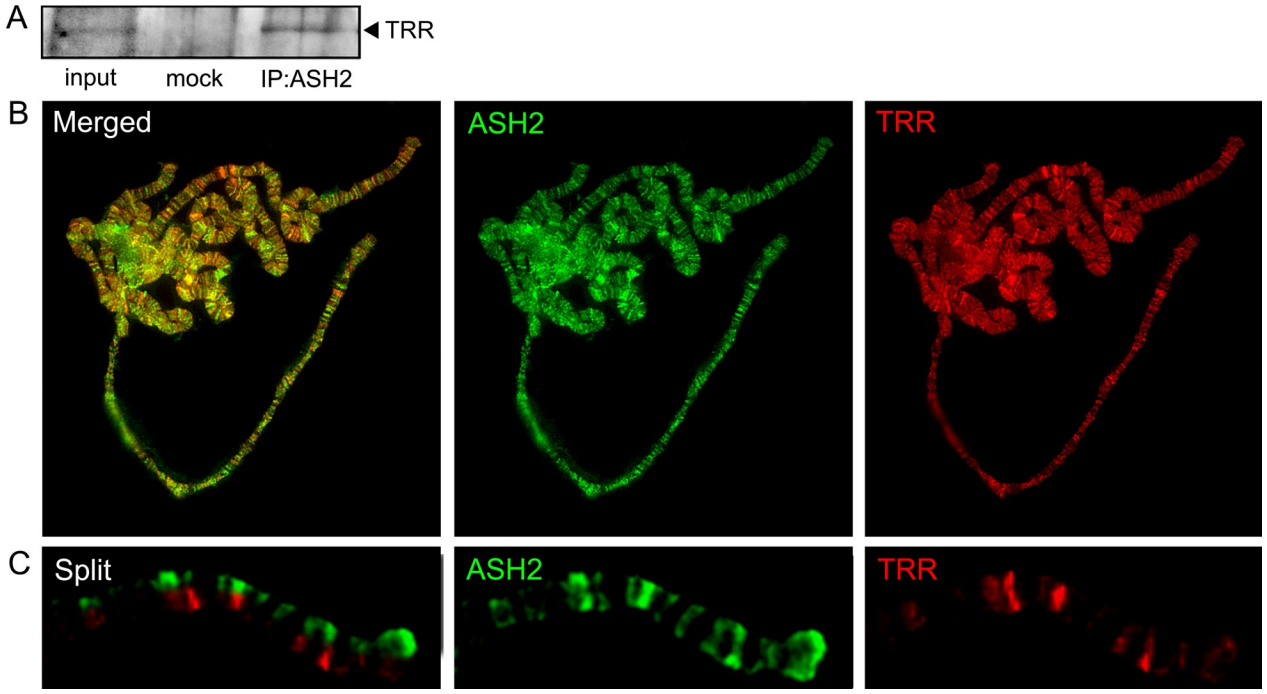

FIGURE 5: Ash2 associates with Trr. (A) Ash2 coimmunoprecipitated with Trr. Anti-Ash2 immunoprecipitations were performed with nuclear extractions from embryos. The input lane shows 10% of the total extract volume used for the coimmunoprecipitation. (B) Ash2 colocalized with Trr on polytene chromosomes from third-instar larvae. The distribution of Ash2 was compared with that of Trr. (C) A magnification of a 2L chromosome arm is shown as a split view, indicating the distribution of Ash2-HA as compared with that of Trr.

contains a phenylalanine/tyrosine-rich (FYRN) domain recently found to be involved in the nuclear proteosomal-independent degradation of the mammalian homologue of Trx (MLL1; Yokoyama *et al.*, 2011). Finally, a differential role for Ash2 regarding Trr and Trx is not unexpected, given that Trr is a highly dynamic protein recruited in response to ecdysone to activate transcription of ecdysone-inducible genes (Sedkov *et al.*, 2003; Johnston *et al.*, 2011).

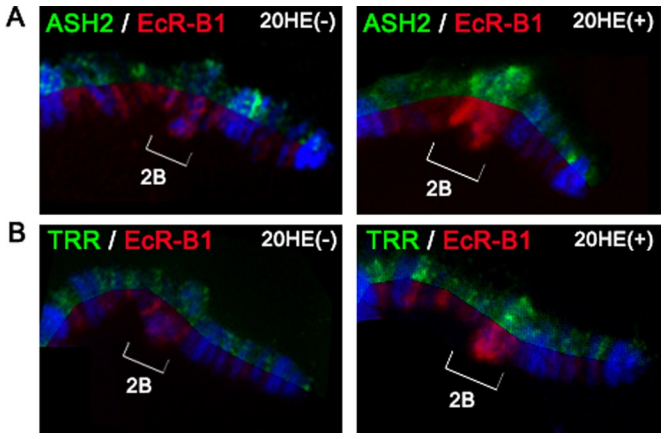

FIGURE 6: Ash2 and Trr are recruited to the cytological region 2B after ectopic ecdysone treatment. Distribution of Ash2 and EcR-B1 (A) and Trr and EcR-B1 (B) at the end of polytene X chromosome from mid-third-instar larvae is shown in a split view. The binding of Ash2, Trr, and EcR is compared at the cytological region 2B (brackets) in the absence (left) or presence (right) of an ectopic ecdysone treatment that caused an early response puff 2B to be formed as a consequence of *BR-C* transcription.

In contrast, Trx is present at promoters and polycomb responsive elements from both transcriptionally active and inactive genes (Papp and Muller, 2006; Schuettengruber *et al.*, 2009; Schwartz *et al.*, 2010). Consistently, it has been demonstrated that recruitment of Trr, but not of Trx, is affected by the absence of EcR (Johnston *et al.*, 2011). In addition, a recent report showed that the protein Cara Mitad (CMI) associates with TRR and EcR-USP, is required for proper trimethylation of H3K4, and needs to bind to chromatin for hormone-stimulated transcription (Chauhan *et al.*, 2012). CMI/Lpt had already been identified as a component of the Trr complex that contains Ash2 (Mohan *et al.*, 2011). Taken together, these results point to the singularity and specificity of Trr-containing complexes involved in EcR responses.

It has been suggested that H3K4me3 may act by recruiting factors that generate a particular architecture at promoters that is critical for optimal transcription (Ardehali *et al.*, 2011). In fact, the functional implications of this histone modification is determined by several effector proteins that bind to the trimethylated H3K4 marks; possible outcomes include regulation of transcription initiation, chromatin remodeling, and modulation of splicing efficiency (Sims *et al.*, 2007; Vermeulen *et al.*, 2007). Moreover, Ash2 and its associated H3K4me3 play a role in transcriptional pausing control (Perez-Lluch *et al.*, 2011). In addition to the mechanisms by which H3K4me3 influence transcription, we can infer that Ash2 regulates the majority of ecdysone-responsive genes by its ability to stabilize Trr. Although additional research is necessary to describe the exact coverage of Trr over ecdysone-inducible genes, the hypothesis that the Ash2 modulation of Trr stabilization has a regulatory role is supported by the colocalization of Ash2 and Trr on polytene chromosomes that we report here, as well as with the previously described overlap of the Trr and EcR polytene chromosome-binding sites (Sedkov *et al.*, 2003).

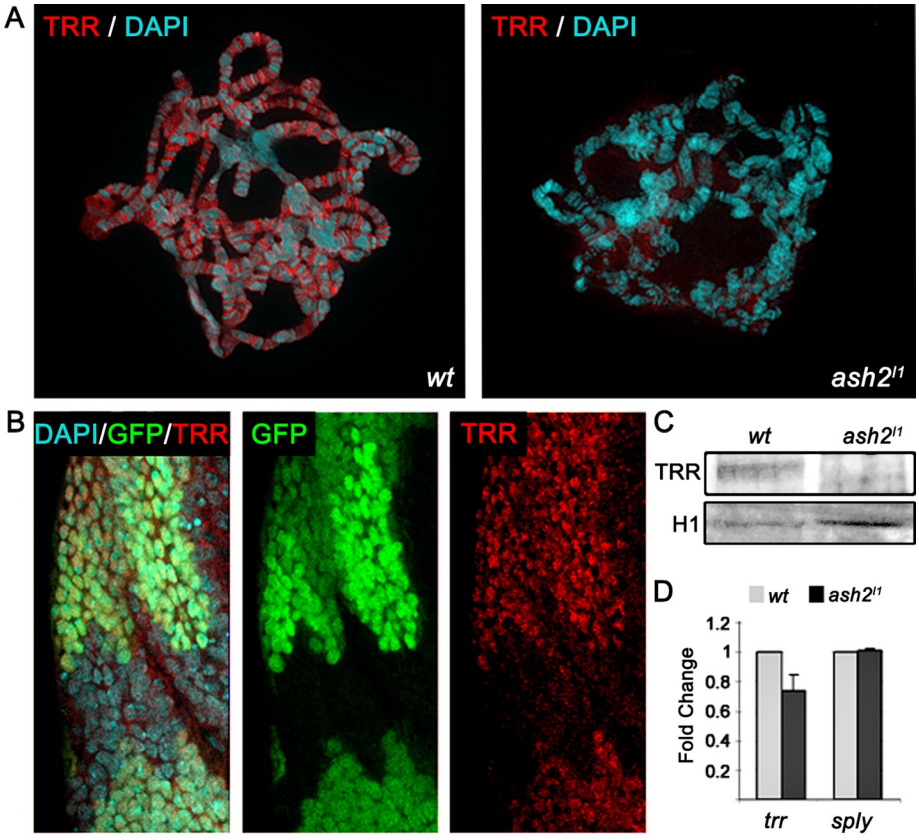

FIGURE 7: Ash2 is required to stabilize Trr. (A) Distribution of Trr on polytene chromosomes from wild-type (left) and *ash2*^{l1} (right) third-instar larvae. (B) Loss of Ash2 dramatically reduced the levels of Trr. Detection of Trr in wild-type (bright green), heterozygous (green), and *ash2*^{l1} homozygous (black) wing disk cells. (C) Detection by Western blot of Trr on larval nuclear extracts of wild-type and *ash2*^{l1}. H1 was used as a loading control. (D) Effect of *ash2* mutation on the expression of *trr*. Wing disk mRNA levels of *trr* was measured by quantitative RT-PCR relative to the control gene *sply*.

Taken together, our work points to a crucial role for Ash2 in activating EcR target genes in *Drosophila*. Our results may also serve as a template to discover whether, in a mechanistically similar manner, nuclear receptors are activated by MLL2, MLL3, and ASH2L in mammals. Further experiments are required to elucidate the specificity of Ash2 in the different complexes and to interpret the complexity of differentiation phenotypes observed in *ash2* mutants.

MATERIALS AND METHODS

Drosophila strains

All *Drosophila* strains and crosses were kept on standard media. The strains used were as follows: *y w; ash2*$^{1124.11}$*/TM6C* (Deak *et al.*, 1997; Amoros *et al.*, 2002), *y w; ash2*^{l1}*/TM6C* (Amoros *et al.*, 2002), *w; UAS-ash2-HA/CyO* (Beltran *et al.*, 2007), *EcR*^{M554fs}/SM6B (Bender *et al.*, 1997), *y w; FRT82Bash2*^{l1}*/TM6C* (Beltran *et al.*, 2003), *y w trr*^{1}*/FM6GFP, y w trr*^{1}*10DFRT18A/FM7C* (Sedkov *et al.*, 2003), *y w hsflp; FRT82BubiGFP/TM6B, w; +; da-gal4, w f*^{36a} *FRT18A/FM6; hsflp /TM6* (Bloomington *Drosophila* Stock Center, Indiana University, Bloomington, IN). *Canton S* was used as the wild-type strain.

To study the interactions between *ash2* and *EcR*, we crossed the strains *w; ash2*$^{1124.11}$*/TM6C* and *w; EcR*^{M554fs}*/CyO; ash2*$^{1124.11}$*/TM6C*. Heterozygous flies for either *ash2*$^{1124.11}$ or *EcR*^{M554fs} were used as controls.

To examine the interactions between *ash2* and *trr*, we crossed males *w; ash2*$^{1124.11}$*/TM6C* with females *y w trr*^{1}*/FM6GFP; +; ash2*$^{1124.11}$*/TM6C* and determined the number of *y w trr*^{1}*/w; +; ash2*$^{1124.11}$ females that reached the adult stage. Heterozygous flies for either *ash2*$^{1124.1}$ or *trr*^{1} were used as controls.

Developmental staging of larvae

To assess the expression of ecdysone-responsive genes and the presence of H3K4me3, we staged wild-type and homozygous *ash2*^{l1} larvae on bromophenol blue–containing media at 25°C and then collected at clear gut stage (~4 h before pupariation) as described (Andres and Thummel, 1994).

Genetic mosaics

Clones mutant for all TrxG genes analyzed in wing imaginal disks from third-instar larvae were obtained by mitotic recombination using the *FLP/FRT* technique (Xu and Rubin, 1993). Larvae of the appropriate genotypes were cultured at 25°C and timed in hours AEL. Heat shock was carried out for 45 min at 37°C (60 ± 12 h AEL) to induce clone formation.

For *ash2*^{l1} mutant clones, *y w; FRT-82Bash2*^{l1}*/TM6C* flies were crossed with *y w hsflp; FRT82BubiGFP/TM6B*.

Clones mutant for *trr*^{1} analyzed in adult structures were obtained by mitotic recombination using the *FLP/FRT* technique by crossing *y w trr*^{1}*10DFRT18A/FM7C* flies with *w f*^{36a} *FRT18A/FM6; hsflp/TM6*. Larvae were cultured at 25°C, and heat shock was performed for 45 min at 37°C (85 ± 12 h AEL).

Antibodies

The following primary antibodies were used: anti–Trx N-terminal antibody N1 (Kuzin *et al.*, 1994), anti-Trr (Sedkov *et al.*, 2003), anti–EcR-B1 (DSHB, AD4.4), anti–EcR-A (DSHB, 15G1a), anti-hemagglutinin (HA; Roche, Indianapolis, IN), anti-V5 (Sigma-Aldrich, St. Louis, MO), anti-H3K4me3 (Millipore, Billerica, MA), anti-H3K4me2 (Upstate, Millipore), anti-H3K4me1 (Diagenode, Denville, NJ), anti-H1, anti-H3 (Abcam, Cambridge, MA), anti-Ash2^{Nt}, and anti-Ash2^{Ct}.

Characterization of the polyclonal Ash2 antibodies generated in our laboratory is shown in Supplemental Figure S1. Specifically, to produce the anti-Ash2^{Nt} antibody, an N-terminal cDNA of 117 base pairs corresponding to the second exon of *ash2* was inserted into a pGEX-2TK expression vector (Invitrogen, Carlsbad, CA) to produce a glutathione *S*-transferase (GST) fusion protein. The GST-tagged protein was purified from bacterial extract using glutathione–Sepharose 4B (GE Healthcare, Piscataway, NJ). GST was cleaved off by incubating with thrombin, and the peptide was purified by high-performance liquid chromatography (AKTA purifier; GE Healthcare) and verified by matrix-assisted laser desorption/ionization–time of flight. The solution of purified peptide was injected into rabbits to generate polyclonal antibodies. To produce the anti-Ash2^{Ct}

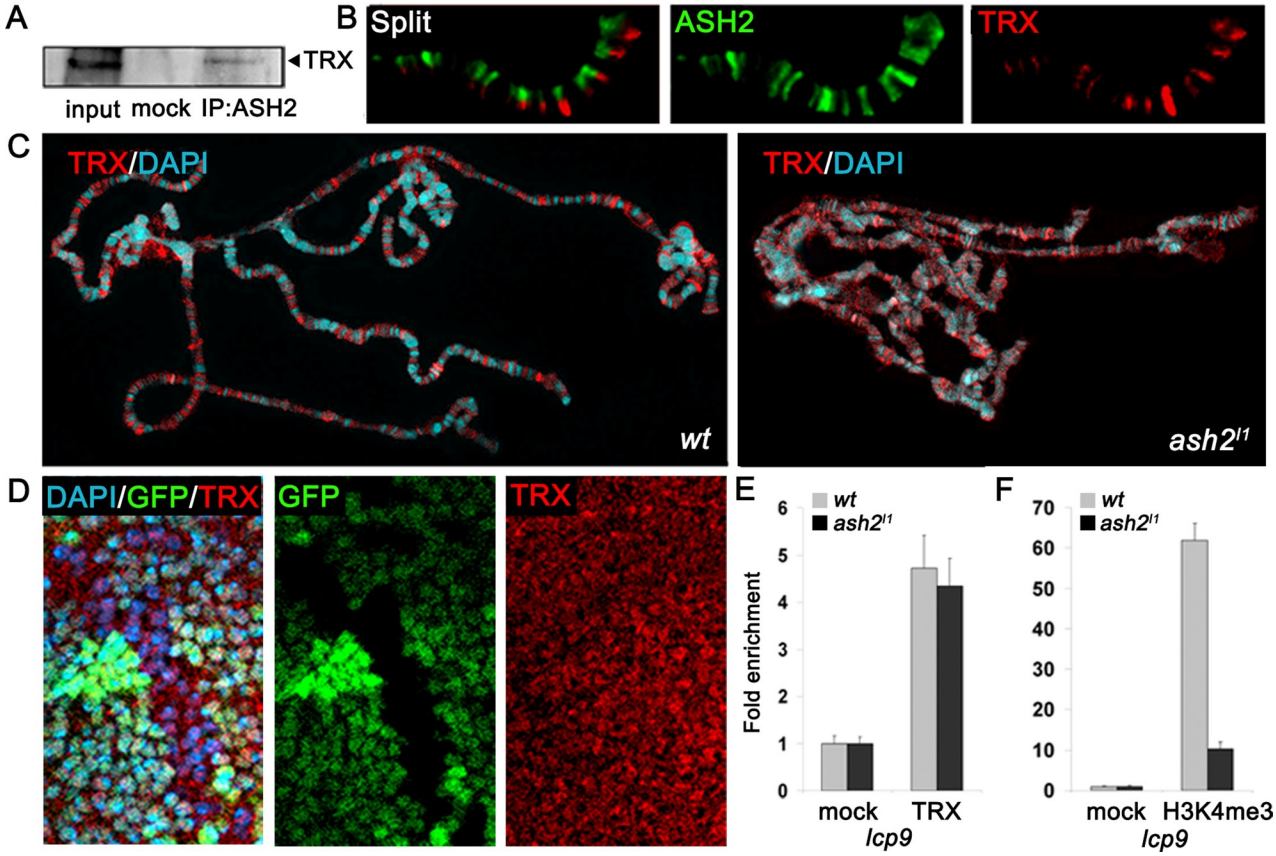

FIGURE 8: Ash2 associates with Trx and facilitates its catalytic activity. (A) Ash2 coimmunoprecipitated with Trx. Anti-Ash2 immunoprecipitations were performed with nuclear extracts from embryos. The input lane shows 10% of the total extract volume used for coimmunoprecipitation. (B) Ash2 colocalized with Trx on polytene chromosomes from third-instar larvae. The distribution of Ash2-HA was compared with that of Trx on a representative region of a wild-type polytene chromosome corresponding to the 2L arm. (C, D) Loss of Ash2 function did not affect Trx levels. (C) Distribution of Trx on polytene chromosomes from wild-type (left) and *ash2*^{l1} (right) third-instar larvae. (D) Trx detected in wild-type (bright green), heterozygous (green), and *ash2*^{l1} homozygous (black) wing disk cells. (E, F) Trx and H3K4me3 levels at the TSS region of *lcp9*, a common target gene of Trx and Ash2. ChIP analysis of wild-type (gray) and *ash2*^{l1} (black) late-wandering larva using Trx (E) and H3K4me3 (F) antibodies. Real-time PCR results were normalized against the mock sample and are depicted as fold enrichment. Error bars represent SEM.

antibody, we inserted a C-terminal cDNA of 383 base pairs corresponding to the fifth and sixth exons of *ash2* into a pPROEX-HTa expression vector (Invitrogen) to produce a fusion protein with 6× histidine (His) residues. A His-tagged protein from bacterial extract was purified using HIS-Select Nickel Affinity Gel (Sigma-Aldrich). The purified peptide solution was injected into rats to generate polyclonal antibodies.

Coimmunoprecipitation and Western blot assays

For coimmunoprecipitation experiments from embryo extracts, 0- to 16-h-old *Drosophila* embryos were decorionated, rinsed extensively with 0.1% Triton X-100, washed two times with 10 mM Tris-HCl (pH 7.5) and then once with nuclear extraction buffer (10% saccharose, 10 mM Tris-HCl, pH 8, 1 mM $CaCl_2$, 0.1 mM phenylmethylsulfonyl fluoride), homogenized, and centrifuged for 5 min at 5000 rpm. The pellet was resuspended in 1 ml of TS buffer (15 mM Tris-HCl, pH 7.5, 60 mM KCl, 2 mM EDTA, and 1 mM dithiothreitol), and centrifuged for 5 min at 5000 rpm. The pellet was resuspended in lysis buffer (100 mM NaCl, 0.1% NP40, 20 mM 4-(2-hydroxyethyl)-1-piperazineethanesulfonic acid, pH 7.9, and a protease inhibitor cocktail tablet) and centrifuged at 13,000 rpm; the supernatant was then collected, diluted 1:4 with RIPA buffer (140 mM NaCl, 10 mM Tris-HCl, pH 8.0, 1 mM EDTA, 1% Triton X-100, 0.1% SDS, 0.1% Na deoxycholate, and protease inhibitors), and incubated with 2 µl of serum antibody on a rotating wheel overnight at 4°C. Complexes were immunoprecipitated with 35 µl of protein–Sepharose A affinity matrix. Samples were run on 8% SDS–PAGE gels and then transferred to polyvinylidene fluoride membranes. The following antibodies were used for Western blots: rabbit anti-Trx (1:1500), rabbit anti-Trr (1:1500), and goat anti-rabbit peroxidase (1:3000).

Immunohistochemistry

Wing imaginal disk staining. Immunohistochemistry was performed according to standard protocols. Primary antibodies used were mouse anti–EcR-B1 (1:50), mouse anti–EcR-A (1:50), rabbit anti-H3K4me3 (1:200), rabbit anti-Trr (1:500), and rabbit anti-Trx (1:200).

Polytene chromosome staining. Salivary glands of wild-type and UAS-*ash2* transgenic flies were dissected in Gohen buffer, fixed for 2 min, and transferred to a solution with acetic acid and formaldehyde for 3 min before squashing to spread the polytene chromosomes. Staining was performed by incubation overnight at 4°C with the

following antibodies: mouse anti-HA (1:200), rat anti-Ash2^{Ct} (1:200), rabbit anti-Ash2^{Nt} (1:200), mouse anti–EcR-B1 (1:5), rabbit anti-Trr (1:500), rabbit anti-Trx (1:200), and rabbit anti-H3K4me3 (1:200).

Preparations were incubated with fluorescein isothiocyanate– or rhodamine red–conjugated secondary antibodies (1:200; Jackson ImmunoResearch Laboratories, West Grove, PA) and then mounted with phosphate-buffered saline/glycerol/4′,6-diamidino-2-phenylindole to stain the DNA.

Ecdysone treatment

For in vivo ecdysone treatment, larvae were synchronized at the second- to third-instar molt and collected 24 h later at mid-L3 stage. Salivary glands were removed and placed into Robb medium. Each gland was divided into two parts, one treated with ecdysone, and the other used as a control. For ecdysone treatment, 20 µM 20-OH-ecdysone (Sigma-Aldrich) was added to the medium, and the lobes of the glands were incubated at 25°C for 2 h. After incubation, ecdysone and control salivary glands were used to prepare polytene chromosome squashes.

Chromatin immunoprecipitation

For qPCR ChIPs, 40 wild-type and *ash2^{l1}* third-instar larvae were fixed. Real-time PCRs were normalized against the mock sample (background control without antibody) and depicted as fold enrichment above the mock.

The larva pool was suspended in 700 µl of sonication buffer and then sonicated in a Branson sonifier. Conditions were established to obtain chromatin fragment lengths of 200–1000 base pairs. Chromatin was centrifuged for 10 min at top speed at 4°C, and the supernatant was recovered. For the input, 10 µl of chromatin were de-cross-linked and purified. Immunoprecipitations were carried out in RIPA buffer. To preclear, 35 µl of 50% (vol/vol) protein A–Sepharose CL4B was added to each immunoprecipitation, and they were incubated for 1.5 h at 4°C on a rotating wheel. Protein A was removed by centrifugation at 3000 rpm for 2 min. A suitable amount of antibody (2 µl for Trx protein and 2 µg for H3K4me3) was added to each chromatin aliquot, and these were incubated on a rotating wheel overnight at 4°C. As a negative control, an aliquot was immunoprecipitated without antibody. Immunocomplexes were recovered by adding 35 µl of 50% (vol/vol) protein A–Sepharose (previously blocked in RIPA or IP/1% bovine serum albumen for 2 h at 4 °C) to the sample and incubating with rocking for 3 h at 4°C. Protein A was washed five times for 10 min each time in 1 ml of RIPA buffer or IP buffer, once in 0.25 M LiCl, 0.5% NP-40, 0.5% sodium deoxycholate, 1 mM Na-EDTA, and 10 mM Tris-HCl (pH 8.0), and twice in TE (1 mM Na-EDTA, 10 mM Tris-HCl, pH 8.0). Protein A was resuspended in 100 µl of TE, and DNase-free RNase at 50 µg/ml was added and incubated for 30 min at 37°C. To purify the immunoprecipitated DNA, samples were adjusted to 0.5% SDS and 500 µg/ml proteinase K and incubated overnight at 65°C. Immunoprecipitated chromatin was purified with Qiagen (Valencia, CA) PCR purification columns, following the manufacturer's instructions. The primers are shown in Table 1.

	Primer
BR-C (+1079 to +1212; isoform M)	FW_5′-TTGACATTTTAAACTGCATT-3′
	RV_5′-AAGTTGTGCATTTGTTTCT-3′
E75A (–1852 to –1751)	FW_5′-ACGAGATACAACTTGGGCTTGGGA-3′
	RV_5′-TGAGGCGAGTGAACTCCTTGGAAA-3′
lcp9 (+143 to +215)	FW_5′-TTGTAAAGAGCGACTCCGA-3′
	RV_5′-CGCGAATATGGTTGGATAG-3′

Coordinates are given relative to the TSS of each target gene.

TABLE 1: Primers for chromatin immunoprecipitation.

	Primer
BR-C	FW_5′-AGGAGATCGGCGACGGAC-3′
	RV_5′-AGGTGTGAGGCTGCCCAG-3′
E75A	FW_5′-GCAGCAGCAGATCGGAATACTC-3′
	RV_5′-CCGACTCAATGCCCGAATCC-3′
trr	FW_5′-TGGCTACAAGGTGAGTCGC-3′
	RV_5′-AACTCGGGCTTGCATCC-3′
rp49	FW_5′-ATGCTAAGCTGTCCACAAATG-3′
	RV_5′-CAGATACTGTCCCTTGAAGC-3′
sply	FW_5′- CTTTCCCGATTCCCGTAGC-3′
	RV_5′-TGACGGGCTTAAGGCAATC-3′

TABLE 2: Primers for qPCR.

RNA extraction, RT-PCR, and real-time PCR

RNA was prepared from wing imaginal disks and fat bodies of *w; ash2^{l1}* and *Canton S* late-third-instar larvae using RNeasy Mini Kit (Qiagen) for RNA extraction from wing imaginal disks and TRIzol reagent (Invitrogen) for RNA extraction from fat bodies, according to the manufacturers' instructions. Quality was assessed in all samples using the Eukaryote Total RNA Nano Assay on a 2100 Bioanalyzer (Agilent Technologies, Santa Clara, CA). Total RNA (1 µg) was used for cDNA synthesis. Reverse transcription was performed using random hexamers and AMW reverse transcriptase (Roche). Real-time PCR was carried out using an ABI PRISM 7500 Sequence Detection System (Applied Biosystems, Foster City, CA), using SYBR Green and standard Applied Biosystems settings. Reactions were run in triplicate in at least two independent experiments. Expression data were normalized to the control genes sply (for wing imaginal disk expression data) or rp49 (for fat body expression data). The primers are shown in Table 2.

Bioinformatics analysis

We considered the GO enrichments identified by DAVID (Huang da *et al.*, 2009) in FAT-filtered biological process and molecular function categories and in the Kyoto Encyclopedia of Genes and Genomes (www.genome.jp/kegg/) pathway.

To produce a graphical distribution for the reads from each sample around the TSS, we calculated the weighted number of reads on each position from 2000 base pairs upstream to 2000 base pairs downstream of the TSS of all genes (according to RefSeq, www.ncbi.nlm.nih.gov/RefSeq/).

ACKNOWLEDGMENTS

We thank E. Blanco for kindly providing bioinformatics support, S. Pérez-Lluch for insightful suggestions, A. Mateo for technical support, and J. Muller for *Drosophila* stocks. We also thank the Confocal Unit of the Universitat de Barcelona Core Facilities (Barcelona, Spain). This project was funded by grants BMC2006-07334, BFU2009-09781, and CSD2007-00008 from the Ministerio de Ciencia e Innovacion, Spain. A.C. was supported by an APIF fellowship from Universitat de Barcelona.

REFERENCES

Adamson AL, Shearn A (1996). Molecular genetic analysis of *Drosophila* ash2, a member of the trithorax group required for imaginal disc pattern formation. Genetics 144, 621–633.

Allis CD *et al*. (2007). New nomenclature for chromatin-modifying enzymes. Cell 131, 633–636.

Amoros M, Corominas M, Deak P, Serras F (2002). The ash2 gene is involved in *Drosophila* wing development. Int J Dev Biol 46, 321–324.

Andres AJ, Thummel CS (1994). Methods for quantitative analysis of transcription in larvae and prepupae. Methods Cell Biol 44, 565–573.

Angulo M, Corominas M, Serras F (2004). Activation and repression activities of ash2 in *Drosophila* wing imaginal discs. Development 131, 4943–4953.

Ardehali MB, Mei A, Zobeck KL, Caron M, Lis JT, Kusch T (2011). *Drosophila* Set1 is the major histone H3 lysine 4 trimethyltransferase with role in transcription. EMBO J 30, 2817–2828.

Badenhorst P, Xiao H, Cherbas L, Kwon SY, Voas M, Rebay I, Cherbas P, Wu C (2005). The *Drosophila* nucleosome remodeling factor NURF is required for ecdysteroid signaling and metamorphosis. Genes Dev 19, 2540–2545.

Bai J, Uehara Y, Montell DJ (2000). Regulation of invasive cell behavior by taiman, a *Drosophila* protein related to AIB1, a steroid receptor coactivator amplified in breast cancer. Cell 103, 1047–1058.

Barski A, Cuddapah S, Cui K, Roh TY, Schones DE, Wang Z, Wei G, Chepelev I, Zhao K (2007). High-resolution profiling of histone methylations in the human genome. Cell 129, 823–837.

Bashirullah A, Lam G, Yin VP, Thummel CS (2007). dTrf2 is required for transcriptional and developmental responses to ecdysone during *Drosophila* metamorphosis. Dev Dyn 236, 3173–3179.

Beckstead R, Ortiz JA, Sanchez C, Prokopenko SN, Chambon P, Losson R, Bellen HJ (2001). Bonus, a *Drosophila* homolog of TIF1 proteins, interacts with nuclear receptors and can inhibit betaFTZ-F1-dependent transcription. Mol Cell 7, 753–765.

Beltran S, Angulo M, Pignatelli M, Serras F, Corominas M (2007). Functional dissection of the ash2 and ash1 transcriptomes provides insights into the transcriptional basis of wing phenotypes and reveals conserved protein interactions. Genome Biol 8, R67.

Beltran S, Blanco E, Serras F, Perez-Villamil B, Guigo R, Artavanis-Tsakonas S, Corominas M (2003). Transcriptional network controlled by the trithorax-group gene ash2 in *Drosophila* melanogaster. Proc Natl Acad Sci USA 100, 3293–3298.

Bender M, Imam FB, Talbot WS, Ganetzky B, Hogness DS (1997). *Drosophila* ecdysone receptor mutations reveal functional differences among receptor isoforms. Cell 91, 777–788.

Berger EM, Dubrovsky EB (2005). Juvenile hormone molecular actions and interactions during development of *Drosophila* melanogaster. Vitam Horm 73, 175–215.

Bialecki M, Shilton A, Fichtenberg C, Segraves WA, Thummel CS (2002). Loss of the ecdysteroid-inducible E75A orphan nuclear receptor uncouples molting from metamorphosis in *Drosophila*. Dev Cell 3, 209–220.

Breen TR, Harte PJ (1991). Molecular characterization of the trithorax gene, a positive regulator of homeotic gene expression in *Drosophila*. Mech Dev 35, 113–127.

Cao F, Chen Y, Cierpicki T, Liu Y, Basrur V, Lei M, Dou Y (2010). An Ash2L/RbBP5 heterodimer stimulates the MLL1 methyltransferase activity through coordinated substrate interactions with the MLL1 SET domain. PLoS One 5, e14102.

Chauhan C, Zraly CB, Parilla M, Diaz MO, Dingwall AK (2012). Histone recognition and nuclear receptor co-activator functions of *Drosophila* Cara Mitad, a homolog of the N-terminal portion of mammalian MLL2 and MLL3. Development 139, 1997–2008.

Christianson AM, King DL, Hatzivassiliou E, Casas JE, Hallenbeck PL, Nikodem VM, Mitsialis SA, Kafatos FC (1992). DNA binding and heteromerization of the *Drosophila* transcription factor chorion factor 1/ultraspiracle. Proc Natl Acad Sci USA 89, 11503–11507.

D'Avino PP, Thummel CS (2000). The ecdysone regulatory pathway controls wing morphogenesis and integrin expression during *Drosophila* metamorphosis. Dev Biol 220, 211–224.

Deak P *et al*. (1997). P-element insertion alleles of essential genes on the third chromosome of *Drosophila* melanogaster: correlation of physical and cytogenetic maps in chromosomal region 86E-87F. Genetics 147, 1697–1722.

Dehe PM *et al*. (2006). Protein interactions within the Set1 complex and their roles in the regulation of histone 3 lysine 4 methylation. J Biol Chem 281, 35404–35412.

Dillon SC, Zhang X, Trievel RC, Cheng X (2005). The SET-domain protein superfamily: protein lysine methyltransferases. Genome Biol 6, 227.

Dou Y, Milne TA, Ruthenburg AJ, Lee S, Lee JW, Verdine GL, Allis CD, Roeder RG (2006). Regulation of MLL1 H3K4 methyltransferase activity by its core components. Nat Struct Mol Biol 13, 713–719.

Dressel U, Thormeyer D, Altincicek B, Paululat A, Eggert M, Schneider S, Tenbaum SP, Renkawitz R, Baniahmad A (1999). Alien, a highly conserved protein with characteristics of a corepressor for members of the nuclear hormone receptor superfamily. Mol Cell Biol 19, 3383–3394.

Eissenberg JC, Shilatifard A (2010). Histone H3 lysine 4 (H3K4) methylation in development and differentiation. Dev Biol 339, 240–249.

Francis VA, Zorzano A, Teleman AA (2010). dDOR is an EcR coactivator that forms a feed-forward loop connecting insulin and ecdysone signaling. Curr Biol 20, 1799–1808.

Freeman MR, Dobritsa A, Gaines P, Segraves WA, Carlson JR (1999). The dare gene: steroid hormone production, olfactory behavior, and neural degeneration in *Drosophila*. Development 126, 4591–4602.

Garen A, Kauvar L, Lepesant JA (1977). Roles of ecdysone in *Drosophila* development. Proc Natl Acad Sci USA 74, 5099–5103.

Gates J, Lam G, Ortiz JA, Losson R, Thummel CS (2004). rigor mortis encodes a novel nuclear receptor interacting protein required for ecdysone signaling during *Drosophila* larval development. Development 131, 25–36.

Gauhar Z, Sun LV, Hua S, Mason CE, Fuchs F, Li TR, Boutros M, White KP (2009). Genomic mapping of binding regions for the Ecdysone receptor protein complex. Genome Res 19, 1006–1013.

Goo YH *et al*. (2003). Activating signal cointegrator 2 belongs to a novel steady-state complex that contains a subset of trithorax group proteins. Mol Cell Biol 23, 140–149.

Guenther MG, Levine SS, Boyer LA, Jaenisch R, Young RA (2007). A chromatin landmark and transcription initiation at most promoters in human cells. Cell 130, 77–88.

Hall BL, Thummel CS (1998). The RXR homolog ultraspiracle is an essential component of the *Drosophila* ecdysone receptor. Development 125, 4709–4717.

Henrich VC, Sliter TJ, Lubahn DB, MacIntyre A, Gilbert LI (1990). A steroid/thyroid hormone receptor superfamily member in *Drosophila* melanogaster that shares extensive sequence similarity with a mammalian homologue. Nucleic Acids Res 18, 4143–4148.

Huang da W, Sherman BT, Lempicki RA (2009). Systematic and integrative analysis of large gene lists using DAVID bioinformatics resources. Nat Protoc 4, 44–57.

Hughes CM *et al*. (2004). Menin associates with a trithorax family histone methyltransferase complex and with the hoxc8 locus. Mol Cell 13, 587–597.

Ingham PW (1983). Differential expression of bithorax complex genes in the absence of the extra sex combs and trithorax genes. Nature 306, 591–593.

Johnston DM, Sedkov Y, Petruk S, Riley KM, Fujioka M, Jaynes JB, Mazo A (2011). Ecdysone- and NO-mediated gene regulation by competing EcR/Usp and E75A nuclear receptors during *Drosophila* development. Mol Cell 44, 51–61.

Justin N, De Marco V, Aasland R, Gamblin SJ (2010). Reading, writing and editing methylated lysines on histone tails: new insights from recent structural studies. Curr Opin Struct Biol 20, 730–738.

King-Jones K, Thummel CS (2005). Nuclear receptors—a perspective from *Drosophila*. Nat Rev Genet 6, 311–323.

Koelle MR, Talbot WS, Segraves WA, Bender MT, Cherbas P, Hogness DS (1991). The *Drosophila* EcR gene encodes an ecdysone receptor, a new member of the steroid receptor superfamily. Cell 67, 59–77.

Krogan NJ, Dover J, Khorrami S, Greenblatt JF, Schneider J, Johnston M, Shilatifard A (2002). COMPASS, a histone H3 (lysine 4) methyltransferase required for telomeric silencing of gene expression. J Biol Chem 277, 10753–10755.

Kuzin B, Tillib S, Sedkov Y, Mizrokhi L, Mazo A (1994). The *Drosophila* trithorax gene encodes a chromosomal protein and directly regulates the region-specific homeotic gene fork head. Genes Dev 8, 2478–2490.

LaJeunesse D, Shearn A (1995). Trans-regulation of thoracic homeotic selector genes of the Antennapedia and bithorax complexes by the trithorax group genes: absent, small, and homeotic discs 1 and 2. Mech Dev 53, 123–139.

Lee JH, Skalnik DG (2005). CpG-binding protein (CXXC finger protein 1) is a component of the mammalian Set1 histone H3-Lys4 methyltransferase complex, the analogue of the yeast Set1/COMPASS complex. J Biol Chem 280, 41725–41731.

Lee JH, Tate CM, You JS, Skalnik DG (2007). Identification and characterization of the human Set1B histone H3-Lys4 methyltransferase complex. J Biol Chem 282, 13419–13428.
Lee S *et al*. (2006). Coactivator as a target gene specificity determinant for histone H3 lysine 4 methyltransferases. Proc Natl Acad Sci USA 103, 15392–15397.
Li CJ, DePamphilis ML (2002). Mammalian Orc1 protein is selectively released from chromatin and ubiquitinated during the S-to-M transition in the cell division cycle. Mol Cell Biol 22, 105–116.
Li T, Bender M (2000). A conditional rescue system reveals essential functions for the ecdysone receptor (EcR) gene during molting and metamorphosis in *Drosophila*. Development 127, 2897–2905.
Miller T, Krogan NJ, Dover J, Erdjument-Bromage H, Tempst P, Johnston M, Greenblatt JF, Shilatifard A (2001). COMPASS: a complex of proteins associated with a trithorax-related SET domain protein. Proc Natl Acad Sci USA 98, 12902–12907.
Milne TA, Briggs SD, Brock HW, Martin ME, Gibbs D, Allis CD, Hess JL (2002). MLL targets SET domain methyltransferase activity to Hox gene promoters. Mol Cell 10, 1107–1117.
Milne TA *et al*. (2005). Menin and MLL cooperatively regulate expression of cyclin-dependent kinase inhibitors. Proc Natl Acad Sci USA 102, 749–754.
Mohan M, Herz HM, Smith ER, Zhang Y, Jackson J, Washburn MP, Florens L, Eissenberg JC, Shilatifard A (2011). The COMPASS family of H3K4 methylases in *Drosophila*. Mol Cell Biol 31, 4310–4318.
Nagy PL, Griesenbeck J, Kornberg RD, Cleary ML (2002). A trithorax-group complex purified from *Saccharomyces cerevisiae* is required for methylation of histone H3. Proc Natl Acad Sci USA 99, 90–94.
Oro AE, McKeown M, Evans RM (1990). Relationship between the product of the *Drosophila* ultraspiracle locus and the vertebrate retinoid X receptor. Nature 347, 298–301.
Oro AE, McKeown M, Evans RM (1992). The *Drosophila* retinoid X receptor homolog ultraspiracle functions in both female reproduction and eye morphogenesis. Development 115, 449–462.
Papp B, Muller J (2006). Histone trimethylation and the maintenance of transcriptional ON and OFF states by trxG and PcG proteins. Genes Dev 20, 2041–2054.
Perez-Lluch S, Blanco E, Carbonell A, Raha D, Snyder M, Serras F, Corominas M (2011). Genome-wide chromatin occupancy analysis reveals a role for ASH2 in transcriptional pausing. Nucleic Acids Res 39, 4628–4639.
Pokholok DK *et al*. (2005). Genome-wide map of nucleosome acetylation and methylation in yeast. Cell 122, 517–527.
Roguev A, Schaft D, Shevchenko A, Pijnappel WW, Wilm M, Aasland R, Stewart AF (2001). The *Saccharomyces cerevisiae* Set1 complex includes an Ash2 homologue and methylates histone 3 lysine 4. EMBO J 20, 7137–7148.
Roy S *et al*. (2010). Identification of functional elements and regulatory circuits by *Drosophila* modENCODE. Science 330, 1787–1797.
Ruthenburg AJ, Allis CD, Wysocka J (2007). Methylation of lysine 4 on histone H3: intricacy of writing and reading a single epigenetic mark. Mol Cell 25, 15–30.
Schneider J *et al*. (2005). Molecular regulation of histone H3 trimethylation by COMPASS and the regulation of gene expression. Mol Cell 19, 849–856.
Schubiger M, Carre C, Antoniewski C, Truman JW (2005). Ligand-dependent de-repression via EcR/USP acts as a gate to coordinate the differentiation of sensory neurons in the *Drosophila* wing. Development 132, 5239–5248.
Schubiger M, Wade AA, Carney GE, Truman JW, Bender M (1998). *Drosophila* EcR-B ecdysone receptor isoforms are required for larval molting and for neuron remodeling during metamorphosis. Development 125, 2053–2062.
Schuettengruber B, Ganapathi M, Leblanc B, Portoso M, Jaschek R, Tolhuis B, van Lohuizen M, Tanay A, Cavalli G (2009). Functional anatomy of polycomb and trithorax chromatin landscapes in *Drosophila* embryos. PLoS Biol 7, e13.
Schwartz YB, Kahn TG, Stenberg P, Ohno K, Bourgon R, Pirrotta V (2010). Alternative epigenetic chromatin states of polycomb target genes. PLoS Genet 6, e1000805.
Sedkov Y, Benes JJ, Berger JR, Riker KM, Tillib S, Jones RS, Mazo A (1999). Molecular genetic analysis of the *Drosophila* trithorax-related gene which encodes a novel SET domain protein. Mech Dev 82, 171–179.
Sedkov Y *et al*. (2003). Methylation at lysine 4 of histone H3 in ecdysone-dependent development of *Drosophila*. Nature 426, 78–83.
Sharma S, De Carvalho DD, Jeong S, Jones PA, Liang G (2011). Nucleosomes containing methylated DNA stabilize DNA methyltransferases 3A/3B and ensure faithful epigenetic inheritance. PLoS Genet 7, e1001286.
Shea MJ, King DL, Conboy MJ, Mariani BD, Kafatos FC (1990). Proteins that bind to *Drosophila* chorion *cis*-regulatory elements: a new C2H2 zinc finger protein and a C2C2 steroid receptor-like component. Genes Dev 4, 1128–1140.
Shearn A, Garen A (1974). Genetic control of imaginal disc development in *Drosophila*. Proc Natl Acad Sci USA 71, 1393–1397.
Shearn A, Rice T, Garen A, Gehring W (1971). Imaginal disc abnormalities in lethal mutants of *Drosophila*. Proc Natl Acad Sci USA 68, 2594–2598.
Shilatifard A (2008). Molecular implementation and physiological roles for histone H3 lysine 4 (H3K4) methylation. Curr Opin Cell Biol 20, 341–348.
Sims RJ 3rd, Millhouse S, Chen CF, Lewis BA, Erdjument-Bromage H, Tempst P, Manley JL, Reinberg D (2007). Recognition of trimethylated histone H3 lysine 4 facilitates the recruitment of transcription postinitiation factors and pre-mRNA splicing. Mol Cell 28, 665–676.
Smith ST, Petruk S, Sedkov Y, Cho E, Tillib S, Canaani E, Mazo A (2004). Modulation of heat shock gene expression by the TAC1 chromatin-modifying complex. Nat Cell Biol 6, 162–167.
Southall SM, Wong PS, Odho Z, Roe SM, Wilson JR (2009). Structural basis for the requirement of additional factors for MLL1 SET domain activity and recognition of epigenetic marks. Mol Cell 33, 181–191.
Steward MM, Lee JS, O'Donovan A, Wyatt M, Bernstein BE, Shilatifard A (2006). Molecular regulation of H3K4 trimethylation by ASH2L, a shared subunit of MLL complexes. Nat Struct Mol Biol 13, 852–854.
Talbot WS, Swyryd EA, Hogness DS (1993). *Drosophila* tissues with different metamorphic responses to ecdysone express different ecdysone receptor isoforms. Cell 73, 1323–1337.
Tsai CC, Kao HY, Yao TP, McKeown M, Evans RM (1999). SMRTER, a *Drosophila* nuclear receptor coregulator, reveals that EcR-mediated repression is critical for development. Mol Cell 4, 175–186.
Tschiersch B, Hofmann A, Krauss V, Dorn R, Korgel G, Reuter G (1994). The protein encoded by the *Drosophila* position- effect variegation suppressor gene Su(var)3–9 combines domains of antagonistic regulators of homeotic gene complexes. EMBO J 13, 163822–3831.
Venkatesh K, Hasan G (1997). Disruption of the IP3 receptor gene of *Drosophila* affects larval metamorphosis and ecdysone release. Curr Biol 7, 500–509.
Vermeulen M *et al*. (2007). Selective anchoring of TFIID to nucleosomes by trimethylation of histone H3 lysine 4. Cell 131, 58–69.
Vogtli M, Elke C, Imhof MO, Lezzi M (1998). High level transactivation by the ecdysone receptor complex at the core recognition motif. Nucleic Acids Res 26, 2407–2414.
Wysocka J, Myers MP, Laherty CD, Eisenman RN, Herr W (2003). Human Sin3 deacetylase and trithorax-related Set1/Ash2 histone H3-K4 methyltransferase are tethered together selectively by the cell-proliferation factor HCF-1. Genes Dev 17, 896–911.
Xu T, Rubin GM (1993). Analysis of genetic mosaics in developing and adult *Drosophila* tissues. Development 117, 1223–1237.
Yao TP, Segraves WA, Oro AE, McKeown M, Evans RM (1992). *Drosophila* ultraspiracle modulates ecdysone receptor function via heterodimer formation. Cell 71, 63–72.
Yokoyama A, Ficara F, Murphy MJ, Meisel C, Naresh A, Kitabayashi I, Cleary ML (2011). Proteolytically cleaved MLL subunits are susceptible to distinct degradation pathways. J Cell Sci 124, 2208–2219.
Yokoyama A, Wang Z, Wysocka J, Sanyal M, Aufiero DJ, Kitabayashi I, Herr W, Cleary ML (2004). Leukemia proto-oncoprotein MLL forms a SET1-like histone methyltransferase complex with menin to regulate Hox gene expression. Mol Cell Biol 24, 5639–5649.